Inorganic Chemistry

Article

pubs.acs.org/IC

Visible-Light-Induced Photooxidation of Ruthenium(II) Complex with 2,2′-Biimidazole-like Ligand by Singlet Oxygen

Zheng-Zheng Li,[†] Yan-Li Niu,[†] Hai-Yun Zhou,[‡] Hsiu-Yi Chao,*[,†] and Bao-Hui Ye*[,†]

[†]MOE Key Laboratory of Bioinorganic and Synthetic Chemistry, School of Chemistry and Chemical Engineering, Sun Yat-Sen University, Guangzhou 510275, China

[‡]Instrumental Analysis and Research Center, Sun Yat-Sen University, Guangzhou 510275, China

Supporting Information

ABSTRACT: Four new ruthenium(II) complexes $[Ru(bpy)_2(TMBiimH_2)](ClO_4)_2$ (**Ru-5**; bpy is 2,2′-bipyridine and $TMBiimH_2$ is 4,5,4′,5′-tetramethyl-2,2′-biimidazole), $[Ru(bpy)_2(L1H_2)](ClO_4)_2{\cdot}H_2O$ (**Ru-6**; $L1H_2$ is 4,5-dimethyl-2-(*N*,*N*-diacetyl)carboximidamide-1*H*-imidazole), $[Ru(bpy)_2(L2H_2)](ClO_4)_2$ (**Ru-7**; $L2H_2$ is N^1,N^1,N^2,N^2-tetrakis-(acetyl)ethanediimidamide), and $[Ru(phen)_2(TMBiimH_2)](ClO_4)_2$ (**Ru-8**; phen is 1,10′-phenanthroline) have been synthesized and characterized. Their photophysical and electrochemical properties have been studied and compared to the previously reported $[Ru(bpy)_2(BiimH_2)](PF_6)_2$ (**Ru-1**), $[Ru(bpy)_2(BbimH_2)](PF_6)_2$ (**Ru-2**), $[Ru(bpy)_2(DMBbimH_2)](PF_6)_2$ (**Ru-3**), and $[Ru(bpy)_2(TMBbimH_2)](PF_6)_2$ (**Ru-4**). Under irradiation with either sunlight or household light in atmosphere, **Ru-5** reacts with molecular oxygen to produce **Ru-6** in an acetonitrile solution with a relatively high concentration and **Ru-7** in a methanol or dilute acetonitrile solution, respectively. The mechanism studies show that singlet oxygen is the reactive oxygen species in the ring-opening reaction and the photooxidation reaction is solvent- and concentration-dependent. The photoreaction product **Ru-6** is an intermediate, which has been isolated and structurally characterized by single-crystal X-ray diffraction. **Ru-6** is stable in the solid state and an acetonitrile solution with a high concentration, but can be further oxidized to **Ru-7** in a methanol or dilute acetonitrile solution.

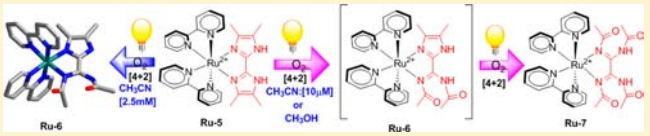

INTRODUCTION

Singlet oxygen ($^1O_2$), molecular oxygen in the excited state and a powerful oxidant, is widely used in organic synthesis, photodynamic therapy for cancer, and photodegradation of dyes.[1,2] It can be produced with varying efficiency as a consequence of quenching of both excited singlet and triplet states of photosensitizers by molecular oxygen. Ruthenium(II) polypyridine and related complexes have been shown to be good candidates for generating singlet oxygen because their long-lived triplet metal-to-ligand charge transfer (^{3}MLCT) excited states could react with molecular oxygen.[3] Therefore, the light-induced reaction of ruthenium polypyridine complexes with DNA in the presence of molecular oxygen has been of interest,[4−6] where singlet oxygen frequently attacks the imidazole group in guanine moiety of DNA, resulting in DNA photocleavage.[7−13] However, many photosensitizers involve imidazole group, which also presents in the biological molecules such as purine and histidine.[14−19] The previous studies show that imidazole and its derivatives can also be photooxidized by singlet oxygen.[20−24] That is to say, the photosensitizer containing imidazole group may react with singlet oxygen when it is used as a $^1O_2$ photosensitizer in the DNA photocleavage and photodynamic therapy. However, the detailed processes are still not well understood.

In our previous studies, a family of four ruthenium(II) 2,2′-biimidazole-like complexes, $[Ru(bpy)_2(BiimH_2)](PF_6)_2$ (**Ru-1**; bpy is 2,2′-bipyridine and $BiimH_2$ is 2,2′-biimidazole), $[Ru(bpy)_2(BbimH_2)](PF_6)_2$ (**Ru-2**; $BbimH_2$ is 2,2′-bibenzimidazole), $[Ru(bpy)_2(DMBbimH_2)](PF_6)_2$ (**Ru-3**; $DMBbimH_2$ is 7,7′-dimethyl-2,2′-bibenzimidazole), and $[Ru(bpy)_2(TMBbimH_2)](PF_6)_2$ (**Ru-4**; $TMBbimH_2$ is 5,6,5′,6′-tetramethyl-2,2′-bibenzimidazole), have been developed as anion sensors, in which the Ru(II)-bpy moiety was utilized as a signaling subunit and the biimidazole ligand was used as a binding site (see Scheme 1).[26−28] They have two acidic N−H protons, with different pK_{a1} values of 7.2 for **Ru-1**,[29] 5.7 for **Ru-2**,[30] 6.2 for **Ru-3**,[27] and 6.8 for **Ru-4**[28] in an acetonitrile−water solution. As part of an ongoing study, $[Ru(bpy)_2(TMBiimH_2)](ClO_4)_2$ (**Ru-5**; $TMBiimH_2$ is 4,5,4′,5′-tetramethyl-2,2′-biimidazole) has been synthesized, where four methyl groups were introduced to the $BiimH_2$ ligand to tune the pK_{a1} value. In the course of crystal growth under atmosphere, we obtained an unexpected product under irradiation with either sunlight or household light. On further investigation we have uncovered a remarkable ring-opening reaction (ROR) via singlet oxygen, in which the initial $TMBiimH_2$ ligand in **Ru-5** was photooxidized to 4,5-dimethyl-2-(*N*,*N*-diacetyl)-carboximidamide-1*H*-imidazole ($L1H_2$), and $[Ru(bpy)_2(L1H_2)](ClO_4)_2{\cdot}H_2O$ (**Ru-6**, see Scheme 1) was obtained in an acetonitrile solution with a relatively high concentration. In this contribution, the photophysical and

Received: June 3, 2013
Published: August 15, 2013

dx.doi.org/10.1021/ic4014043 | *Inorg. Chem.* 2013, 52, 10087−10095

Scheme 1. Structures of Cations in Ru-1 to Ru-8

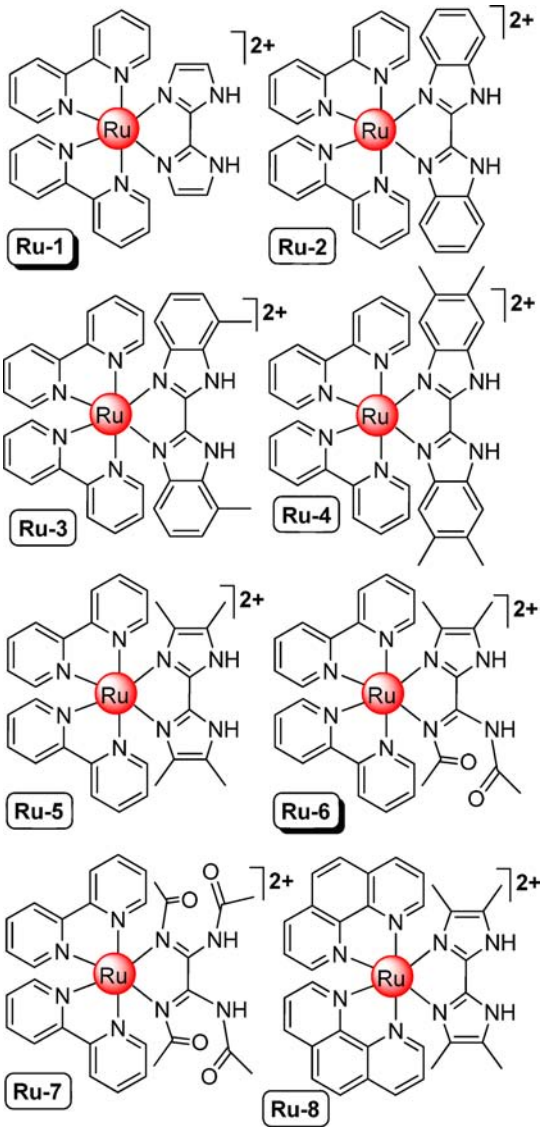

photochemical properties of **Ru-5** have been investigated to illuminate its photoreactivity. The detailed photooxidation of **Ru-5** by molecular oxygen has been studied in acetonitrile and methanol solutions under household light irradiation at room temperature. Furthermore, the product of the photoreaction, **Ru-6**, has also been isolated and structurally characterized by single-crystal X-ray diffraction. This would provide direct evidence for the mechanism of the chemiluminescence of 2,4,5-triphenylimidazole (lophine), which is a long-standing problem.[31] In addition, we also found that $L1H_2$ ligand in **Ru-6** would be further oxidized to N^1,N^1,N^2,N^2- tetrakis-(acetyl)-ethanediimidamide ($L2H_2$) in a methanol solution and $[Ru(bpy)_2(L2H_2)](ClO_4)_2$ (**Ru-7**) can be produced. This result is quite different from those of the reactions between imidazole derivatives and singlet oxygen in a methanol solution, where a methanol adduct was formed.[32] On the basis of these findings, we propose a mechanism for the photooxidation reaction of **Ru-5** with singlet oxygen in various conditions. Moreover, an analogous complex $[Ru(phen)_2(TMBiimH_2)](ClO_4)_2$ (**Ru-8**; phen is 1,10′-phenanthroline) was also synthesized, and the photoreaction with molecular oxygen under visible light irradiation at room temperature was examined in different solvents. These studies could also help to understand the mechanism of imidazole ring breakdown in DNA and enzymes by photosensitized oxidation.

EXPERIMENTAL SECTION

Materials. 4,5,4′,5′-Tetramethyl-2,2′-biimidazole was bought from Sigma-Aldrich and used without purification. Other reagent grade chemicals obtained from commercial sources were used as received. HPLC acetonitrile and deionized water were used in UV, luminescence, and electrochemical measurements. DMSO-d_6 was used in NMR experiments. $[Ru(bpy)_2Cl_2]\cdot 2H_2O$, $[Ru(phen)_2Cl_2]\cdot 2H_2O$,[33] and $[Ru(bpy)_3](ClO_4)_2$[34] were prepared by the literature methods.

Synthesis of ***Ru-5****.* $[Ru(bpy)_2Cl_2]\cdot 2H_2O$ (0.26 g, 0.5 mmol), $TMBiimH_2$ (0.11 g, 0.6 mmol), and ethylene glycol (14 mL) were added into a 50 mL three neck flask. The mixture was magnetically stirred and refluxed for 4 h under argon protection, and then cooled to room temperature and filtered. Concentrated hydrochloric acid (2 mL, 11 M) and saturated aqueous $NaClO_4$ solution (20 mL) were added to the filtrate, respectively. A red precipitate was obtained and purified on a neutral alumina column chromatography with a mixture of CH_3CN/toluene (5:1, v/v) as an eluent. The main red band was collected. The solvent was removed under reduced pressure to give a red powder. The yield was 70%. Anal. Calcd for $C_{30}H_{30}Cl_2N_8O_8Ru$: C 44.90, H 3.77, N 13.96. Found: C 44.76, H 3.86, N 14.37. ESI-MS: m/z = 602 $[M - 2ClO_4 - H]^+$, 301 $[M - 2ClO_4]^{2+}$. FT-IR (KBr, cm^{-1}): 3430 br, 2923 m, 1608 m, 1460 m, 1366 m, 1258 m, 1092 vs, 768 m, 625 m. ^1H NMR (300 MHz, DMSO-d_6) δ 12.67 (*s*, 2H, N−H), 8.73 (dd, 4H, bpy), 8.10 (t, 2H, bpy), 8.00 (t, 2H, bpy), 7.93 (d, J = 5.3 Hz, 2H, bpy), 7.72 (d, J = 5.3 Hz, 2H, bpy), 7.63 (t, 2H, bpy), 7.37 (t, 2H, bpy), 2.16 (s, 6H, H_2TMbiim), 1.08 (s, 6H, H_2TMbiim). ^{13}C NMR (75.5 MHz, DMSO-d_6): δ 158.2, 157.0, 151.3, 151.0, 143.4, 135.6, 135.2, 131.6, 129.2, 126.9, 126.7, 123.5, 123.3, 11.2, 9.3.

Synthesis of ***Ru-6****.* An acetonitrile solution (20 mL) containing **Ru-5** (42 mg, 0.05 mmol) was magnetically stirred at room temperature for 2 h. Then, the solution was filtered, and the filtrate was kept at room temperature to volatilize the solvent under irradiation with either sunlight or household light. The deep red crystals of **Ru-6** were obtained after 2 days. The yield was 54%. Anal. Calcd for $C_{30}H_{32}Cl_2N_8O_{11}Ru$: C 42.26, H 3.78, N 13.14. Found: C 41.84, H 3.56, N 13.45. ESI-MS: m/z = 635 $[M - 2ClO_4 - H]^+$, 593 $[M - 2ClO_4 - COCH_3]^+$, 317 $[M - 2ClO_4]^{2+}$, 297 $[M - 2ClO_4 - COCH_3 + H]^{2+}$. IR (KBr cm^{-1}): 3427 br, 1729 m, 1602 m, 1582 m, 1520 s, 1445 m, 1385 vs, 1248 m, 1152 m, 1098 vs, 763 m, 623 m. ^1H NMR (300 MHz, DMSO-d_6) δ 13.96 (s, br, 1H, N−H), 11.22 (s, br, 1H, N−H), 8.79 (m, 4H, bpy), 8.64 (d, J = 5.3 Hz, 1H, bpy), 8.21 (m, 2H, bpy), 8.06 (m, 2H, bpy), 7.85 (d, J = 5.6 Hz, 1H, bpy), 7.79 (t, 1H, bpy), 7.67 (m, 2H, bpy), 7.55 (d, J = 5.6 Hz, 1H, bpy), 7.43 (m, 2H, bpy), 2.24 (s, 3H, CH_3), 2.15 (s, 3H, CH_3), 1.43 (s, 3H, CH_3), 1.20 (s, 3H, CH_3). ^{13}C NMR (75.5 MHz, DMSO-d_6): δ 185.8, 171.5, 160.3, 158.0, 157.4, 157.3, 157.2, 152.3, 151.9, 151.2, 151.0, 145.5, 140.5, 139.1, 136.2, 135.8, 135.6, 134.7, 127.2, 127.1, 126.8, 125.6, 123.8, 123.6, 123.1, 122.5, 27.5, 25.1, 18.9, 18.6.

Synthesis of ***Ru-7****.* A MeOH solution (500 mL) containing **Ru-5** (5.0 mg, 6.22 μmol) was magnetically stirred and irradiated with a 5 W lamp from ca. 5 cm distance at room temperature for 12 h. The solvent was removed under reduced pressure. The raw product was purified on a silica gel column chromatography with a mixture of CH_3CN/H_2O/KNO_3 (sat.) (50:2:1, v/v) as an eluent. The main red band was collected. The solvent was removed under reduced pressure to give a red powder. The yield was 90%. Anal. Calcd for $C_{30}H_{30}Cl_2N_8O_{12}Ru$: C 41.58, H 3.49, N 12.93. Found: C 41.87, H 3.76, N 12.86. ESI-MS: m/z = 667 $[M - 2ClO_4 - H]^+$, 623 $[M - 2ClO_4 - COCH_3]^+$, 583 $[M - 2ClO_4 - COCH_3 + H]^+$, 292 $[M - 2ClO_4 - COCH_3 + 2H]^{2+}$. IR (KBr cm^{-1}): 3365 m, 3226 m, 3071 m, 2919 vs, 2856 m, 1707 m, 1642 m, 1602 m, 1521 m, 1380 vs, 1251 m, 1093 m, 1023 m, 780 m. ^1H NMR (300 MHz, DMSO-d_6) δ 11.75 (s, 2H, N−H), 8.75 (d, J = 8.4 Hz, 2H, bpy), 8.68 (d, J = 8.4 Hz, 2H, bpy), 8.38 (d, J = 5.1 Hz, 2H, bpy), 8.20 (t, 2H, bpy), 7.99 (t, 2H, bpy), 7.75 (t, 2H, bpy), 7.48 (d, J = 5.4 Hz, 2H, bpy), 7.39 (t, J = 6.6 Hz, 2H, bpy), 2.22 (s, 6H,

dx.doi.org/10.1021/ic4014043 | *Inorg. Chem.* 2013, 52, 10087−10095

H_2L2), 1.23 (s, 6H, H_2L2). ^{13}C NMR (75.5 MHz, DMSO-d_6): δ 181.7, 171.4, 157.3, 157.1, 151.9, 151.1, 150.8, 135.9, 135.6, 127.2, 126.6, 123.5, 123.2, 26.5, 25.8.

Synthesis of ***Ru-8***. The title complex was synthesized by a procedure similar to that of **Ru-5**. The yield was 76%. Anal. Calcd for $C_{34}H_{30}Cl_2N_8O_8Ru$: C 48.01, H 3.55, N 13.17. Found: C 48.35, H 3.74, N 13.26. ESI-MS: m/z = 651 $[M - 2ClO_4 - H]^+$, 326 $[M - 2ClO_4]^{2+}$. ^1H NMR (300 MHz, DMSO-d_6) δ 8.69 (d, J = 8.2 Hz, 2H, phen), 8.52 (d, J = 8.2 Hz, 2H, phen), 8.38 (d, J = 5.3 Hz, 2H, phen), 8.27 (m, 4H, phen), 8.03 (dd, 2H, phen), 7.95 (d, J = 5.3 Hz, 2H, phen), 7.53 (dd, 2H, phen), 1.96 (s, 6H, H_2TMbiim), 0.75 (s, 6H, H_2TMbiim). ^{13}C NMR (75.5 MHz, DMSO-d_6): δ 153.0, 152.7, 148.8, 147.9, 146.3, 135.3, 134.6, 134.4, 132.2, 129.9, 127.7, 127.4, 125.9, 125.4, 10.8, 9.3.

Physical Measurements. Elemental (C, H, and N) analyses were performed on an Elementar Vario EL analyzer. Electrospray ionization mass spectra (ESI-MS) were obtained on a Thermo LCQ DECA XP mass spectrometer. The FT-IR spectra were recorded from KBr pellets in the range 400−4000 cm^{-1} on a Nicolet 330 FT-IR spectrometer. ^1H NMR spectra were obtained on a Varian Mercury-Plus 300 spectrometer. Electronic absorption spectra were obtained on a PERSEE TU-1901 UV−vis spectrophotometer. Luminescence spectra were recorded on a Shimadzu RF-5301PC spectrofluorophotometer. Emission lifetimes were obtained on a FLS920 fluorescence lifetime and steady state spectrometer, and a 500 kHz laser beam at 405 nm was used as light source. All instrument parameters, such as the incident and emergent slit width (0.2 mm for incident and emergent slit) and scanning speed (dwell time, 0.5 s; step, 0.5 nm), were fixed for all measurements, and all samples were loaded as soon as possible and sealed in small quartz cells for measurements. NMR, UV, and luminescence spectra were recorded at 298 K. A 5 W household electric energy saving lamp (YPZ 230/5−2u, Foshan Electric Lighting Co., Ltd.) was used as light source with a ca. 5 cm distance to the reaction solution.

Electrochemistry. Electrochemical measurements were carried out on a CHI-630C electrochemistry system in an acetonitrile solution. A three-electrode assembly comprising a glassy carbon working electrode, a Pt auxiliary electrode, and a nonaqueous $Ag/AgNO_3$ reference electrode was used. The cyclic voltammetric (CV) and square wave voltammetric (SWV) measurements were carried out in an acetonitrile solution of the complex (0.001 mol dm^{-3}), and the concentration of the supporting electrolyte ($TBAPF_6$) was maintained at 0.1 mol dm^{-3}. Argon was bubbled into the solution for 10 min, and the glassy carbon electrode was polished with an alumina/water slurry before measurement. A scan rate of 100 mV s^{-1} was employed for all measurements. The potentials were referenced against the $Ag/AgNO_3$ electrode, which under the given experimental conditions gave a value of $E_{1/2}$ = 0.07 V for the Fc/Fc^+ couple. The $E_{1/2}$ values were determined from CV using the equation $E_{1/2} = 0.5(E_{pc} + E_{pa})$, where E_{pc} and E_{pa} were cathodic and anodic potentials, respectively, and also directly obtained from the peak values of SWV curves.

Quantum Yield Measurements for Complexes. Quantum yields were determined in freeze−thaw−pump degassed solutions of **Ru-5**, **Ru-6**, **Ru-7**, and **Ru-8** by a relative method using $[Ru(bpy)_3]^{2+}$ in the same solvent as the standard.[35] The quantum yield was calculated by the following equation:[36]

$$\Phi_r = \Phi_{std}\frac{A_{std}}{A_r}\frac{I_r}{I_{std}}\frac{\eta_r^2}{\eta_{std}^2}$$

Here, Φ_r and Φ_{std} are the quantum yields of unknown and standard samples (Φ_{std} = 0.062 in CH_3CN and 0.045 in CH_3OH at 298 K with λ_{ex} = 450 nm),[35] A_r and A_{std} are the solution absorbance at the excitation wavelength (λ_{ex}), I_r and I_{std} are the integrated emission intensities, and η_r and η_{std} are the reflective indices of the solvents. Experimental error in the reported luminescence quantum yield was about 20%.

Singlet Oxygen ($^1O_2$) Quantum Yields (Φ_Δ). Quantum yields for singlet oxygen generation in air-saturated MeCN/MeOH were determined by monitoring the photooxidation of 1,3-diphenylisobenzofuran (DPBF) sensitized by the Ru complexes.[19,37] The absorbance of DPBF was adjusted around 1.0 at 414 nm in air saturated MeCN/MeOH, and the absorbance of the sensitizers was adjusted to 0.2 at the irradiation wavelength. The photooxidation of DPBF was monitored at the interval of 5 s. The quantum yields of singlet oxygen generation (Φ_Δ) were calculated by a relative method using Rose Bengal (RB, Φ_Δ^{std} = 0.42 and 0.76 in air-saturated MeCN and MeOH, respectively)[38,39] as the reference. The quantum yield Φ_Δ was calculated by the following equation:

$$\Phi_\Delta^{unk} = \Phi_\Delta^{std}\frac{m^{unk}F^{std}}{m^{std}F^{unk}}$$

Here superscripts unk and std designate Ru complexes and RB, respectively, m is the slope of a plot of difference in change in absorbance of DPBF (at 414 nm) with the irradiation time, and F is the absorption correction factor, which is given by $F = 1 - 10^{-A}$ (absorbance at the irradiation wavelength). Experimental error for the reported quantum yield was about 15%.

Rate Constants (k_q) of Singlet Oxygen Quenching by Ru Complexes. Values of k_q in different solvents were evaluated by the Stern−Volmer analysis of the $^1O_2$ NIR phosphorescence signals (1270 nm) as a function of the concentration of the Ru complex (0−20 μM).[40] RB (20 μM) was employed as standard sensitizer for determining the k_q values of the Ru complex in various solvents. RB was excited at 547 nm, and the Ru complexes do not absorb in this region. A linear relationship between the ratio of the signals observed in the absence (I^o) and in the presence (I^Q) of quencher and the quencher concentration [Q] should be observed. The k_q may be calculated from the slope of the Stern−Volmer plot ($K_{SV} = k_q\tau_0$), where τ_0 in the given solution is known (63 μs in CH_3CN and 12 μs in CH_3OH).[40] The experimental results were the average of three independent series of measurements. Experimental error for the reported rate constant was about 15%.

$$I^o/I^Q = 1 + K_{SV}[Q] = 1 + k_q\tau_0[Q]$$

Kinetics of Photooxidation. Quartz cuvettes with a 1 cm path length and a 3 cm^3 volume were used for all measurements. For UV−vis measurements, absorption spectra of a 40 μM **Ru-5** in acetonitrile or methanol solution were measured under irradiation with a 5 W lamp in a distance of ca. 1 cm. The interval was 20 s during a period of 6 min. The equation $\ln(C_t/C_0) = -k_{obs} \times t$, where C_t, C_0, k_{obs}, and t stand for the concentration of **Ru-5** at reaction time (t), the initial concentration, pseudo-first-order rate constant, and irradiation time (t), respectively, was used to determine the k_{obs}.[41]

Single-Crystal X-ray Crystallography. The diffraction intensities for **Ru-6** were collected at 293 K on a Bruker Smart Apex CCD diffractometer with graphite-monochromated Mo Kα radiation (λ = 0.710 73 Å). Absorption corrections were applied using SADABS.[42] The structure was solved by direct methods and refined with full-matrix least-squares technique using the SHELXS-97 and SHELXL-97 programs, respectively.[43,44] Anisotropic thermal parameters were applied to all nonhydrogen atoms. The organic hydrogen atoms were generated geometrically. The hydrogen atoms of the water molecules were located from difference maps and refined with isotropic temperature factors. The crystal data and the details of data collection and refinement for **Ru-6** are summarized in Table 1. Selected bond distances and angles are listed in Table S1 in the Supporting Information.

RESULTS AND DISCUSSION

Synthesis and Characterization. The synthetic routes for complexes **Ru-5**, **Ru-6**, and **Ru-7** are outlined in Scheme 2. Complex **Ru-5** was obtained by the reaction of $TMBiimH_2$ with $Ru(bpy)_2Cl_2$ in ethylene glycol for 4 h under Ar atmosphere in a moderate yield (70%). It was characterized by ^1H NMR, ^{13}C NMR, IR, and positive ESI-MS spectroscopy (see Figures S1−S3 in the Supporting Information). Satisfactory elemental analysis was also obtained (see Experimental Section). The ^1H NMR spectrum of **Ru-5** in DMSO-d_6 displays two peaks at 1.08

dx.doi.org/10.1021/ic4014043 | Inorg. Chem. 2013, 52, 10087−10095

Table 1. Crystallographic Data for Ru-6

molecular formula	$C_{30}H_{32}Cl_2N_8O_{11}Ru$
M_r	852.61
cryst syst	monoclinic
space group	$P2_1/c$
a/Å	8.483(4)
b/Å	19.513(10)
c/Å	21.032(10)
β/°	94.393(8)
V/Å^3	3471.1(3)
Z	4
D_c (g cm^{-3})	1.632
μ (mm^{-1})	0.677
data/restraints/params	4161/10/459
R1[a] [$I > 2\sigma(I)$], wR2[b] (all data)	0.0903, 0.3099
GOF on F^2	1.023
$\Delta\rho_{max}/\Delta\rho_{min}$ (e Å^{-3})	1.64/1.22

[a] $R1 = \sum||F_o| - |F_c||/\sum|F_o|$. [b] $wR2 = [\sum w(F_o^2 - F_c^2)^2/\sum w(F_o^2)^2]^{1/2}$.

and 2.16 ppm, which are assigned to the resonance of protons on two kinds of methyl groups. The chemical shift at 12.6 ppm is attributed to N−H on the $TMBiimH_2$ ligand. The ^{13}C NMR spectrum of **Ru-5** also exhibits two peaks at 11.2 and 9.3 ppm for the resonance of two kinds of methyl groups in the $TMBiimH_2$ ligand. The ESI-MS spectrum of **Ru-5** shows its monocation $[M - 2ClO_4 - H]^+$ and dication $[M - 2ClO_4]^{2+}$ at m/z = 602 and 301, respectively.

During the course of growing crystals of **Ru-5** from an acetonitrile solution in atmosphere, an unexpected product **Ru-6** was obtained. Single-crystal X-ray analysis revealed that one of the imidazole rings was cleaved and two acetyl groups were formed (*vide infra*). This implied that the ROR took place under a mild condition and encouraged us to re-examine the reaction. When a 2.5 mM **Ru-5** acetonitrile solution was exposed to atmosphere under either sunlight or household light at room temperature for 2 days, complex **Ru-6** was obtained in the yield of 54%. The ^1H NMR spectrum of **Ru-6** in DMSO-d_6 shows four peaks at 1.21, 1.42, 2.15, and 2.24 ppm, indicating the presence of four different methyl groups and a low symmetry in **Ru-6**. The peaks at 1.21 and 1.42 ppm may be assigned to the methyl groups (C21 and C28, *vide infra*) close to the pyridine rings, because of the effect of current ring of the pyridine rings. Four peaks at 27.5, 25.1, 18.9, and 18.6 ppm corresponding to the four methyl groups were also observed in the ^{13}C NMR spectrum. Moreover, the C=C resonance peaks of the imidazole ring at 140.5 and 139.1 ppm and two carbonyl resonance peaks at 185.8 and 171.5 ppm indeed show that only one of the imidazole rings was oxidated to two acetyl groups. These are good agreement with the single crystal X-ray structural analysis (*vide infra*). The IR spectrum of **Ru-6** exhibits a moderate peak at 1729 cm^{-1}, which suggests the formation of carbonyl group (see Figure S4 in the Supporting Information). The ESI-MS spectrum of **Ru-6** shows its monocation $[M - 2ClO_4 - H]^+$ and dication $[M - 2ClO_4]^{2+}$ at m/z = 635 and 317, respectively (see Figure S5 in the Supporting Information).

When a 10 μM **Ru-5** methanol solution was irradiated with a 5 W lamp in atmosphere at room temperature for 12 h, surprisingly, another complex, **Ru-7**, was isolated in the yield of 90% after purification on a silica gel column chromatography. The ESI-MS spectrum of **Ru-7** shows its monocation $[M - 2ClO_4 - H]^+$ and a stable fragment $[M - 2ClO_4 - 2COCH_3 + H]^+$ at m/z = 667 and 583, respectively (see Figure 1), in which a series of isotopic peaks with different intensity ratio are in agreement with the calculated isotope peaks for the corresponding species. The IR spectrum of **Ru-7** exhibited a moderate peak at 1707 cm^{-1}, which could be attributed to the characteristic stretching of carbonyl group (see Figure S5 in the Supporting Information). The ^1H NMR spectrum of **Ru-7** in DMSO-d_6 shows the peaks of protons for two types of methyl groups at 1.23 and 2.22 ppm, which are downfield from those of **Ru-5** (see Figure S6 in the Supporting Information). In addition, there is one singlet with the chemical shift at 11.7 ppm, which is attributed to the resonance of N−H on the $L2H_2$ ligand. Two methyl and two carbonyl resonance peaks at 26.5 and 25.8 ppm, and 181.7 and 171.4 ppm were also observed, respectively. These observations indicate that **Ru-5** and **Ru-7** have a high symmetry in comparison to **Ru-6**. Thus, for the formation of **Ru-7**, two imidazole rings in **Ru-5** are cleaved with the excision of the C=C bonds, and four acetyl groups are formed (see Scheme 2).

Crystal Structure of Ru-6. The crystal structure of **Ru-6** has been determined by X-ray crystallography. It crystallizes in the $P2_1/c$ space group. Each asymmetric unit contains one $[Ru(bpy)_2(L1H_2)]^{2+}$ cation, two ClO_4^- counteranions, and one water molecule. Figure 2 clearly shows that the precursor $TMBiimH_2$ ligand of **Ru-5** is oxidized to $L1H_2$ ligand, in which one of the imidazole rings is cleaved with the excision of the C=C bond and two acetyl groups are formed. The C−O bond distances (1.16 and 1.22 Å) indicate their double bond

Scheme 2. Synthetic Pathway for Complexes Ru-5, Ru-6, and Ru-7

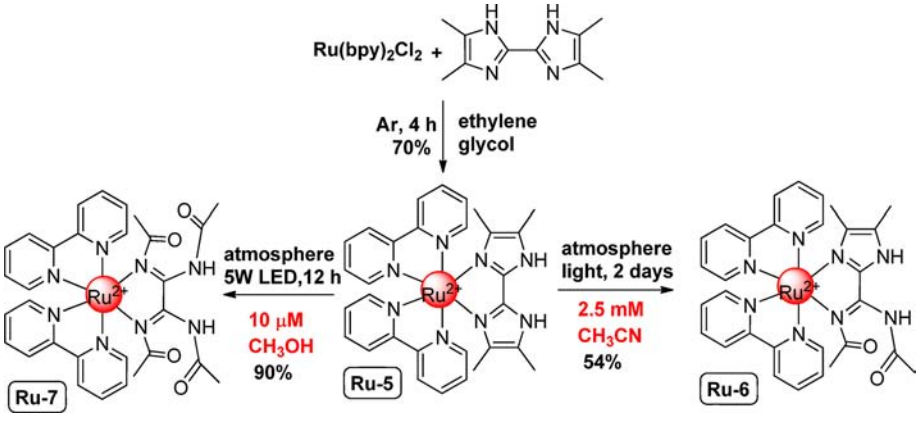

dx.doi.org/10.1021/ic4014043 | Inorg. Chem. 2013, 52, 10087−10095

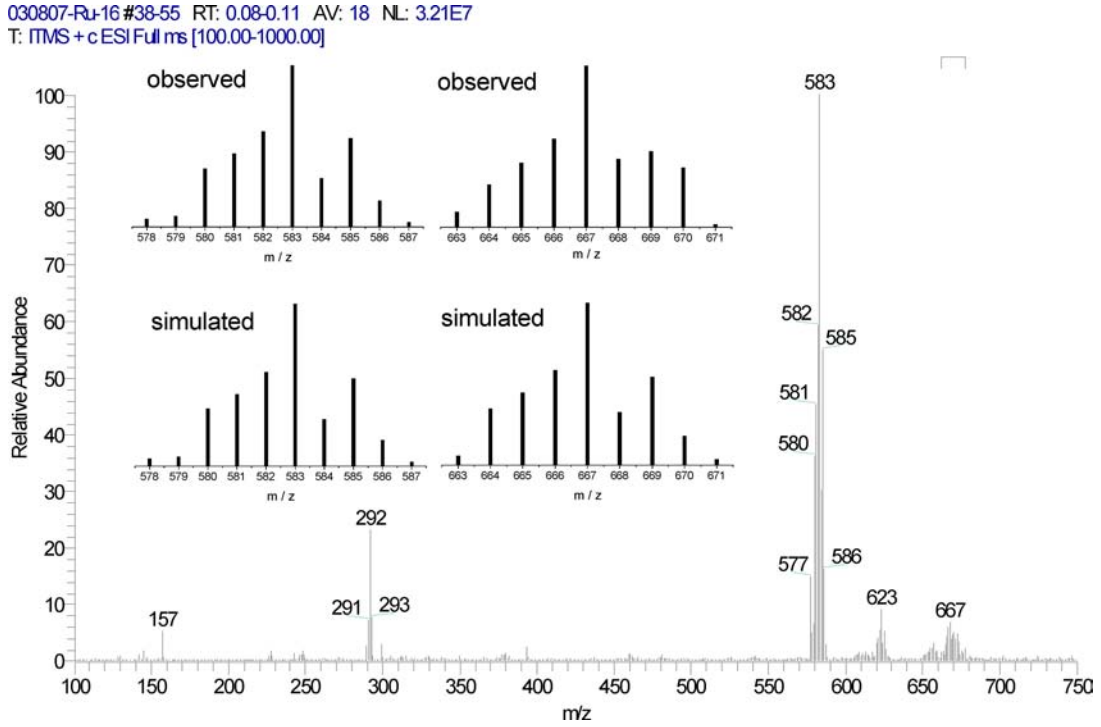

Figure 1. ESI-MS of **Ru-7** in acetonitrile solution. Inset: Amplification of the mass spectra at m/z = 667 and 583, and the calculation for $[M - 2ClO_4 - H]^+$ and $[M - 2ClO_4 - 2COCH_3 - H]^+$.

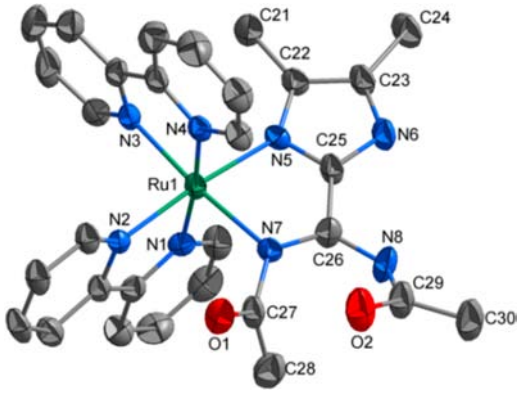

Figure 2. View of the structure of cation in **Ru-6**. Selected bond distances (Å) and angles (deg): Ru1–N5 = 2.079(6), Ru1–N7 = 2.098(6), C25–N5 = 1.31(1), C25–N6 = 1.35(1), C26–N7 = 1.31(1), C26–N8 = 1.36(1), C27–N7 = 1.44(1), C29–N8 = 1.39(1), C27–O1 = 1.16(1), C29–O2 = 1.22(1); N5–Ru1–N7 = 78.3(2), N7–C26–N8 = 128.0(8), C26–N7–C27 = 124.4(7), C26–N8–C29 = 127.2(8).

character. The C26–N7 bond distance (1.31 Å) is shorter than that of C27–N7 (1.44 Å), indicating that the former has double bond character. Each Ru(II) ion is coordinated by two bpy and one $L1H_2$ ligand in a distorted octahedral geometry. The bond distances of Ru1–N5 (2.079 Å) and Ru1–N7 (2.098 Å) are slightly shorter than those reported in the Ru(II) complexes bearing $TMBiimH_2$ ligand (2.114–2.224 Å).[45] The bond angle of N5–Ru1–N7 (78.3°) is slightly larger than those in the Ru(II) complexes bearing $TMBiimH_2$ ligand (75.5 and 77.2°).[45] Furthermore, the N6 atom in the imidazole ring is hydrogen bonding to a water molecule with the distance of N6···O1w *ca.* 2.73 Å; the N8 atom is hydrogen-bonding to the O10 atom in one of the perchlorate anions with a distance of N8···O10 *ca.* 3.05 Å. In addition, the C21 and C28 atoms on methyl groups locate on the pyridine ring planes with 3.2 and 3.5 Å distances, respectively.

Photophysical and Electrochemical Properties. In order to understand why only complex **Ru-5** reacts with molecular oxygen under irradiation with either sunlight or household light in atmosphere at room temperature,[25−31] systematic observations in physical and chemical properties of complexes **Ru-1** to **Ru-7** are performed. Table 2 lists the photophysical and electrochemical data for complexes **Ru-1** to **Ru-8** and $[Ru(bpy)_3]^{2+}$ in CH_3CN. Figure 3 shows the absorption spectra of complexes **Ru-5**, **Ru-6**, **Ru-7**, and **Ru-8** in acetonitrile. Complexes **Ru-5** to **Ru-7** display a strong absorption band at *ca.* 290 nm, which is attributed to the $\pi-\pi^*$ transition of bpy ligand. The 338 nm absorption band for **Ru-5** and **Ru-6** can be assigned to the $\pi-\pi^*$ transition of imidazole ligand. The bands at 483 nm for **Ru-5**, 460 nm for **Ru-6**, 479 nm for **Ru-7**, and 480 nm for **Ru-8** are assigned to the Ru d–bpy/phen π^* transition according to the Rillema's report.[29] The electron density in Ru center of **Ru-5** is higher than those of **Ru-1** to **Ru-4**, due to a stronger σ-donor ability of $TMBiimH_2$ ligand. Thus, the ^{1}MLCT band of **Ru-5** displays a larger red shift compared with those of **Ru-1** to **Ru-4**.

As shown in Figure 4, **Ru-7** is almost nonemissive in an acetonitrile solution at room temperature. In sharp contrast, **Ru-5** exhibits strong photoluminescence at 646 nm with an emissive quantum yield of 0.0083 in acetonitrile at room temperature, which is twice and 7-fold stronger than those of **Ru-1** and **Ru-6**, respectively. The quantum yield of **Ru-8** is 0.0071 in acetonitrile at room temperature. The emission bands of **Ru-1** to **Ru-8** are red-shifted, compared to the 605 nm emission band of $[Ru(bpy)_3]^{2+}$ (λ_{ex} = 450 nm), indicating they have lowered energy of the ^{3}MLCT excited state. This is in good agreement with the red shift of ^{1}MLCT bands in the absorption spectra. By fitting of their emission decay curves to

dx.doi.org/10.1021/ic4014043 | *Inorg. Chem.* 2013, 52, 10087−10095

Table 2. Photophysical and Electrochemical Data of Ru-1 to Ru-8 and $[Ru(bpy)_3]^{2+}$ in Acetonitrile at 298 K

complex	abs λ_{max} (nm)	λ_{em} (nm)	Φ_r (× 10^3)	τ/ns	E_{ox}[a]/V	E_{red}[a]/V	Φ_Δ (× 10)	k_q (×10^{-6}, M^{-1} s^{-1})
Ru-1	290, 341, 475	638[b]	4.5	111[d]	0.71	−1.86, −2.14, −2.24	2.3 (3.4[e])	1.62 (0.33[e])
Ru-2	290, 330, 348, 465	624[b]	2.8	102[d]	0.78	−1.82, −2.08, −2.19	2.7 (3.0[e])	1.64 (0.50[e])
Ru-3	290, 332, 349, 462	617[b]	2.8		0.74	−1.80, −2.06, −2.18		
Ru-4	290, 343, 363, 474	623[b]	3.8		0.74	−1.82, −2.08, −2.20		
Ru-5	291, 313, 338, 483	646[b]	8.3 (12.0[e])	263[d]	0.64	−1.97, −2.17, −2.28	3.6 (4.5[e])	1.97 (0.46[e])
Ru-6	290, 338, 460	644[b]	1.3 (2.7[e])	95[d]	0.86	−1.63, −1.96	1.7 (2.6[e])	1.56 (0.38[e])
Ru-7	292, 479	644[b]	0.56	ND[f]	0.70	−1.89, −2.15	ND[f]	ND[f]
Ru-8	265, 305, 426, 480	652[b]	7.1 (10.0[e])	244[d]	0.67	−1.88, −2.12, −2.32	3.0 (4.4[e])	1.74 (0.50[e])
$[Ru(bpy)_3]^{2+}$[c]	287, 453	605	62 (45[e])	860	0.97	−1.65, −1.84, −2.10	5.7 (8.1[e])[g]	2.75[g]

[a]Versus $Ag/AgNO_3$, $E_{1/2}(Fc/Fc^+)$ = 0.07 V. [b]λ_{ex} = 470 nm. [c]Ref 35. [d]Measured in 50 μM acetonitrile. [e]Measured in CH_3OH solution. [f]Too weak to detect. [g]Ref 46.

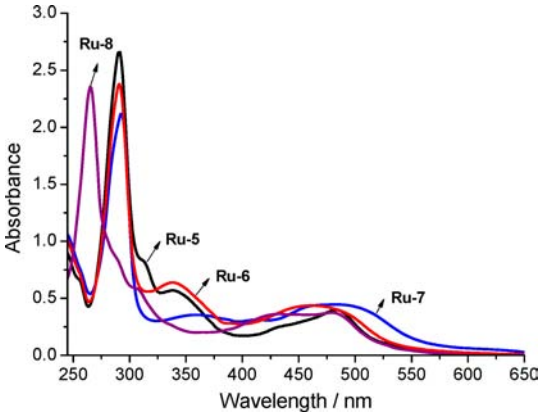

Figure 3. UV-vis spectra of **Ru-5**, **Ru-6**, and **Ru-7** (40 μM) in acetonitrile.

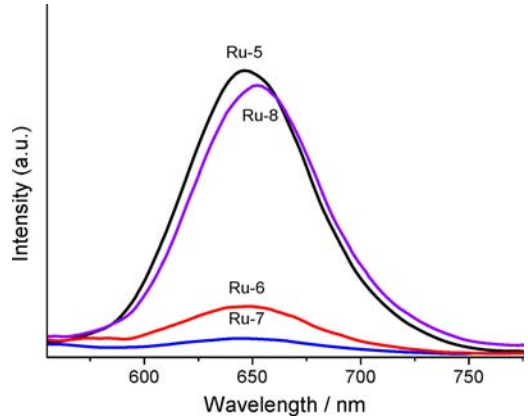

Figure 4. Emission spectra of **Ru-5**, **Ru-6**, and **Ru-7** (40 μM) in acetonitrile (λ_{ex} = 470 nm).

single-exponential functions, the lifetimes of the ^{3}MLCT excited states are 263 ns for **Ru-5**, 95 ns for **Ru-6**, 244 ns for **Ru-8**, 111 ns for **Ru-1**, and 102 ns for **Ru-2** (see Figures S7−S11 in the Supporting Information). The quantum yields and lifetimes of complexes **Ru-1** to **Ru-8** are lower than those of $[Ru(bpy)_3]^{2+}$ (Φ_r = 0.062 and τ = 860 ns).[35] This could be due to the strong acidity of the N−H protons on the $BiimH_2$-like ligands that provides a nonradiative deactivation pathway to the spin-forbidden ^{3}MLCT excited state.[47] It is worth noting that **Ru-5** and **Ru-8** have the longer luminescence lifetime of ^{3}MLCT excited state among **Ru-1** to **Ru-8**. The relatively longer lifetimes of **Ru-5** and **Ru-8** in the ^{3}MLCT excited state make them susceptible to quenching by O_2, generating of the active singlet oxygen.

The redox activities of complexes **Ru-5**, **Ru-6**, **Ru-7**, and **Ru-8** have been examined in an acetonitrile solution using cyclic voltammetry (CV) and square wave voltammetry (SWV) (see Table 2 and Figures S12−S16 in the Supporting Information). Complexes **Ru-5** and **Ru-8** display one-electron oxidation with $E_{1/2}$ = 0.64 and 0.67 V for their $Ru^{2+/3+}$ couple, which are the lowest value among **Ru-1** to **Ru-7** and $[Ru(bpy)_3]^{2+}$. It could be rationalized by the fact that the $TMBiimH_2$ ligand has stronger σ-donor ability and results in the increase of electron density in Ru center.[48] The largest red shift of the ^{1}MLCT bands observed for **Ru-5** and **Ru-8** in the absorption spectrum also supports this hypothesis. In addition, complex **Ru-5** is found to undergo three successive one-electron reductions in the potential window from 1.0 to −2.6 V, which could be assigned to the reduction of bpy and $TMBiimH_2$ ligands. On the contrary, complexes **Ru-6** and **Ru-7** bearing acetyl groups exhibit poor electrochemical behavior (broad, irreversible peaks).[9]

Photoreaction. When a **Ru-5** acetonitrile solution was exposed to atmosphere under irradiation with household light at room temperature, the unexpected product **Ru-6** was obtained in a moderate yield, in which one of the imidazole rings was cleaved and two new acetyl groups were formed. This prompted us to study the ROR mechanism. The ring cleavage reaction occurs at the substituted carbon−carbon double bond in the imidazole ring. These sites have increased electrophilicity because of the introduction of the four electron-donating methyl group to the $BiimH_2$ ligand compared to the other ligands. Moreover, the relatively long-lived triplet excited state of **Ru-5** (263 ns) compared to those of **Ru-1** (111 ns) and **Ru-2** (102 ns) suggests that it may be a good photosensitizer for generation of $^1O_2$ upon irradiation of an air-saturated acetonitrile solution.[10,49] Control experiments (Ar-saturated solution or in the dark) showed that both molecular oxygen and light are essential for the reaction. The presence of DMSO had negligible effects on the photooxidation reaction, ruling out the involvement of O_2^-. Furthermore, upon addition of histidine or NaN_3, the well-known scavenger of $^1O_2$, the photocleavage reaction was inhibited effectively, demonstrating that $^1O_2$ is the main reactive oxygen species in the photooxidation reaction.[50] This can also be further confirmed by the observation of the phosphorescence emission of $^1O_2$ at 1270 nm (*vide infra*).

Upon photoexcitation, the singlet excited states of **Ru-5** are populated and followed by a fast intersystem crossing leading to the formation of the MLCT excited state with a dominant triplet character. The quenching of ^{3}MLCT excited state by molecular oxygen may occur via energy transfer to generate $^1O_2$. Singlet oxygen functions as a powerful electrophile to

dx.doi.org/10.1021/ic4014043 | Inorg. Chem. 2013, 52, 10087−10095

Scheme 3. Proposed Reaction Mechanism for Ru-5 and O_2 under Irradiation with a 5 W lamp

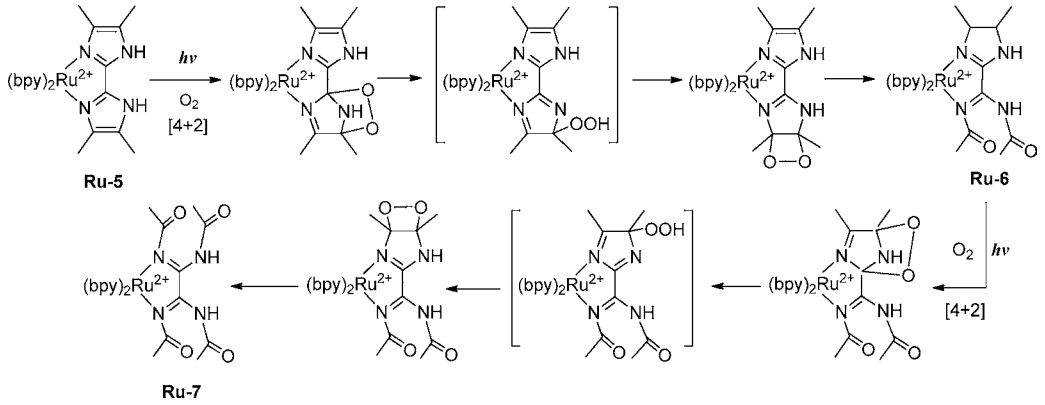

attack the C═C bond with the higher electron density to form an endoperoxide via a [4 + 2] cycloaddition, which decomposes to a hydroperoxide and then forms an epidioxetane. Subsequently, the epidioxetane is converted into *N,N′*-diacetylamidine (see Scheme 3).[31] The molecular structure of product **Ru-6** reveals that the C═C bond of one of the imidazole rings of **Ru-5** is cleaved to yield an *N,N′*-diacetylamidine derivative. This is in good agreement with the previously hypothetical mechanism for lophine, in which the C_4═C_5 bond of 4,5-epidioxide is cleaved into *N,N′*-dibenzoylbenzamidine accompanied by the emission of light.[31] Therefore, the mechanism study on the formation of **Ru-6** would provide the significant information for understanding the chemiluminescence of lophine and photocleavage of DNA.

The photoreaction of **Ru-5** in a dilute methanol solution affording complex **Ru-7** prompted us to study the photoreaction in different solvents with various concentrations. Four **Ru-5** solutions [2.5 mM in an acetonitrile (A), 2.5 mM in a methanol (B), 10 μM in an acetonitrile (C), and 10 μM in a methanol (D)] were irradiated with a 5 W lamp in atmosphere at room temperature, and the reaction products were monitored by ESI-MS spectra during the time course from the beginning to 64 h. For solution A, ESI-MS spectra showed the characteristic peaks of **Ru-6** at m/z = 635 $[M - 2ClO_4 - H]^+$ and 593 $[M - 2ClO_4 - COCH_3]^+$ appeared and gradually increased, and that of **Ru-5** at m/z = 602 decreased during the period from the beginning to 4 h. Beyond that, the peak at m/z = 602 almost disappeared, indicating that **Ru-5** was completely converted into **Ru-6**. By extending the reaction time to 64 h, the peaks for **Ru-6** at 635 and 593 were still intense, but the peaks for **Ru-7** at m/z = 667 $[M - 2ClO_4 - H]^+$ and 623 $[M - 2ClO_4 - COCH_3]^+$ with weak intensities appeared, demonstrating that **Ru-6** was the major product with a small amount of **Ru-7** during this period. For solution **B**, the mixture of **Ru-5** and **Ru-6** were observed during the reaction time from the beginning to 4 h. However, the characteristic peaks of **Ru-7** at m/z = 623 and 499 $[M - 2ClO_4 - 4COCH_3 + 3H]^+$ appeared and gradually increased in 8 h, and only the peaks for **Ru-7** were detected beyond 16 h. These observations indicate that **Ru-6** is the major product before 16 h and **Ru-7** is predominant after 16 h. This is different from the observation in solution **A**, and can be due to the solvent effect.[51]

To understand the solvent effect on the reaction, the triplet quantum yields of **Ru-5** were measured in various solvents. The Φ_r is 0.012 in CH_3OH, that is larger than that obtained from CH_3CN (0.0083). To evaluate the efficiency of the photosensitized singlet oxygen generation in various solvents, the $^1O_2$ generation quantum yields (Φ_Δ) of **Ru-5** were determined in air-saturated MeCN/MeOH with RB (Φ_Δ = 0.42 in CH_3CN and 0.76 in CH_3OH)[38,39] as the standard and DPBF as the trapping agent of $^1O_2$. The $\Phi_\Delta$of **Ru-5** was measured to be 0.36 in CH_3CN and 0.45 in CH_3OH (see Figure S17 in the Supporting Information). This is consistent with the report by Tanielian and co-workers,[51] in which the quenching of $[Ru(bpy)_3]^{2+}$ by molecular oxygen is solvent-dependent and the quantum yield for generation of $^1O_2$ in methanol (0.87) is larger than that in acetonitrile (0.77). The rate constants of singlet oxygen quenching by the Ru complexes were evaluated by the Stern−Volmer analysis of the $^1O_2$ NIR phosphorescence (1270 nm) signals as a function of the concentration of **Ru-5**. The Stern−Volmer plots of $^1O_2$ quenching by **Ru-5** in CH_3CN and CH_3OH were linear (see Figure S18 in the Supporting Information). Therefore, the values of k_q were calculated from the slopes of the plots. The k_q is 1.97×10^6 M^{-1} s^{-1} in CH_3CN and 0.46×10^6 M^{-1} s^{-1} in CH_3OH; this is consistent with the literature.[40]

For solutions C and D, only the peaks at m/z = 634 and 593 were observed in 15 min, indicating that **Ru-5** was completely converted into **Ru-6** within 15 min and this transformation was faster than those observed in solutions **A** and **B**. After 2 h, the peaks of **Ru-7** at m/z = 623 and 583 appeared; **Ru-6** and **Ru-7** species coexisted until 8 h. After that, **Ru-7** was the major product.

From the above observations, the predominant photoreaction mechanism has been proposed as shown in Scheme 3. **Ru-6** is an intermediate in the reaction; it is stable in the solid state and in acetonitrile with a relatively high concentration. However, it can further react with $^1O_2$ and be transformed into **Ru-7** in a methanol or dilute acetonitrile solution. This also implies that the photooxidation reaction is concentration-dependent because the lifetime of the ^{3}MLCT excited state decreases as the concentration of complex in solution increases.[52] It is worth noting that the second step ring-opening reaction is very slow compared to the first step, because of the shorter luminescence lifetime of **Ru-6** (95 ns).

Moreover, the photoreaction of **Ru-8** with molecular oxygen was also observed under irradiation with visible light in atmosphere and monitored by ESI-MS spectrum in CH_3CN/CH_3OH. Similar cases with **Ru-5** were also observed. In high concentration CH_3CN (2.5 mM), only one of imidazole rings was oxidated and two acetyl groups were formed with the characteristic peak at m/z = 682 (analogous to **Ru-6**) after irradiation of 32 h. In dilute CH_3CN solution (10 μM), the oxidation of two imidazole rings occurred and the characteristic

dx.doi.org/10.1021/ic4014043 | *Inorg. Chem.* 2013, 52, 10087−10095

peaks at m/z = 716 and 672 (analogous to **Ru-7**) were observed after irradiation of 32 h. The observations indicate that the reaction of **Ru-8** with molecular oxygen is concentration dependent. In CH_3OH solution, the peaks at m/z = 672 and 630 were observed after 4 h, indicating that the oxidation of two imidazole rings is the major product and the photoreaction is also solvent dependent.

The changes in UV−vis absorption spectra of **Ru-5** (40 μM) in an acetonitrile or methanol solution upon irradiating with a 5 W lamp are shown in Figures 5 and S18 in the Supporting Information, respectively. The MLCT absorption band at 483 nm shifts to 460 nm, and the band at 313 nm decreases concomitant with the increase of the band at 338 nm. During this course, a well-defined isosbestic point at 323 nm is observed, suggesting that only two species coexist in the equilibrium. By investigating the relationship between the concentration change of **Ru-5** and irradiation time, the k_{obs} values can be determined as 3.59×10^{-3} s^{-1} in acetonitrile and 1.99×10^{-2} s^{-1} in methanol, respectively. This indicates that the photoreaction of **Ru-5** in methanol is faster than that in acetonitrile.

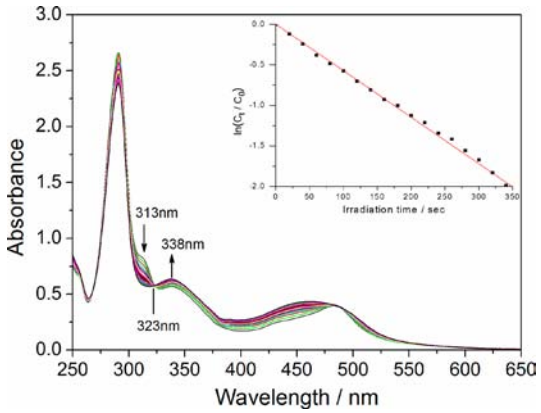

Figure 5. Absorption spectra of **Ru-5** (40 μM) in acetonitrile upon irradiating with a 5W lamp for 0−10 min. The plot of the logarithm of absorbance at 313 nm as a function of time is shown in the inset.

CONCLUSIONS

Four new ruthenium complexes **Ru-5**, **Ru-6**, **Ru-7**, and **Ru-8** have been synthesized and characterized. Their photophysical and electrochemical properties have been studied. **Ru-5** reacts with singlet oxygen, producing **Ru-6** and **Ru-7** depending on the solvents and concentrations. **Ru-6** is an intermediate during the photoreaction and is stable in the solid state as well as an acetonitrile solution with high concentration, but can be further converted into **Ru-7** in methanol and dilute acetonitrile solutions. These studies could help to understand the mechanism of the chemiluminescence of lophine and photocleavage of DNA.

ASSOCIATED CONTENT

Supporting Information

Crystallographic information in CIF format. ESI-MS, IR, ^{1}H NMR, SWV curves for **Ru-5**, **Ru-6**, **Ru-7**, and **Ru-8**; the decay curves for **Ru-1**, **Ru-2**, **Ru-5**, **Ru-6**, and **Ru-8**; the plots of singlet oxygen quantum yield measurements, as well as the Stern−Volmer analysis for quenching of singlet oxygen in CH_3CN and CH_3OH; UV−vis spectra of photooxidation reaction of **Ru-5** in CH_3OH; the selective bond distances and angles for **Ru-6**. This material is available free of charge via the Internet at http://pubs.acs.org. The deposition number CCDC 926090 contains the supplementary crystallographic data for complex **Ru-6**. These data can be obtained free of charge from The Cambridge Crystallographic Data Centre via www.ccdc.cam.ac.uk/data_request/cif.

AUTHOR INFORMATION

Corresponding Author

*E-mail: zhaoxy@mail.sysu.edu.cn (H-Y.C); cesybh@mail.sysu.edu.cn (B-H.Y).

Notes

The authors declare no competing financial interest.

ACKNOWLEDGMENTS

This work was supported by the NSF of China (21071154, 21272284, 20971131), the DPF of MOE of China (No. 0171110004), and the Guangdong NSF (S2012010010566).

REFERENCES

(1) (a) Schweitzer, C.; Schmidt, R. *Chem. Rev.* **2003**, *103*, 1685. (b) De-Rosa, M. C.; Crutchley, R. J. *Coord. Chem. Rev.* **2002**, *233*−*234*, 351. (c) Clennan, E. L.; Pace, A. *Tetrahedron* **2005**, *61*, 6665. (d) Ogilby, P. R. *Chem. Soc. Rev.* **2010**, *39*, 3181.

(2) (a) Dolmans, D. E. J. G.; Fukumura, D.; Jain, R. K. *Nat. Rev. Cancer* **2003**, *3*, 380. (b) Celli, J. P.; Spring, B. Q.; Rizvi, I.; Evans, C. L.; Samkoe, K. S.; Verma, S.; Pogue, B. W.; Hasan, T. *Chem. Rev.* **2010**, *110*, 2795. (c) Lovell, J. F.; Liu, T. W. B.; Chen, J.; Zheng, G. *Chem. Rev.* **2010**, *110*, 2839.

(3) (a) Juris, A.; Balzani, V.; Barigelletti, F.; Campagna, S.; Belser, P.; von Zelewsky, A. *Coord. Chem. Rev.* **1988**, *84*, 85. (b) Baranoff, E.; Collin, J.-P.; Flamigni, L.; Sauvage, J.-P. *Chem. Soc. Rev.* **2004**, *33*, 147. (c) Medlycott, E. A.; Hanan, G. S. *Chem. Soc. Rev.* **2005**, *34*, 133. (d) Wong, K. M.-C.; Yam, V. W.-W. *Coord. Chem. Rev.* **2007**, *251*, 2477. (e) Zhao, Q.; Li, F.; Huang, C. *Chem. Soc. Rev.* **2010**, *39*, 3007. (f) Ruggi, A.; van Leeuwen, F. W. B.; Velders, A. H. *Coord. Chem. Rev.* **2011**, *255*, 2542.

(4) Erkkila, K. E.; Odom, D. T.; Barton, J. K. *Chem. Rev.* **1999**, *99*, 2777.

(5) *DNA and RNA Binders: from Small Molecules to Drugs*; Demeunynck, M., Bailly, C., Wilson, W. D., Eds.; Wiley-VCH: Weinheim, Germany, 2003; Vol. *1*; p 146.

(6) Marcelis, L.; Ghesquiere, J.; Garnir, K.; Kirsch-De, M, A.; Moucheron, C. *Coord. Chem. Rev.* **2012**, *256*, 1569.

(7) Hergueta-Bravo, A.; Jimenez-Hernandez, M. E.; Montero, F.; Oliveros, E.; Orellana, G. *J. Phys. Chem. B* **2002**, *106*, 4010.

(8) Evans, S. E.; Grigoryan, A.; Szalai, V. A. *Inorg. Chem.* **2007**, *46*, 8349.

(9) Williams, B. R.; Dalton, S. R.; Skiba, M.; Kim, S. E.; Shatz, A.; Carroll, P. J.; Burgmayer, S. J. N. *Inorg. Chem.* **2012**, *51*, 12669.

(10) Sun, Y.; Joyce, L. E.; Dickson, N. M.; Turro, C. *Chem. Commun.* **2010**, *46*, 2426.

(11) Zhou, Q.-X.; Lei, W.-H.; Chen, J.-R.; Li, C.; Hou, Y.-J.; Wang, X.-S.; Zhang, B.-W. *Chem.—Eur. J.* **2010**, *16*, 3157.

(12) (a) Du, K.-J.; Wang, J.-Q.; Kou, J.-F.; Li, G.-Y.; Wang, L.-L.; Chao, H.; Ji, L.-N. *Eur. J. Med. Chem.* **2011**, *46*, 1056. (b) Sun, J.; Wu, S.; Chen, H.-Y.; Gao, F.; Liu, J.; Ji, L.-N.; Mao, Z.-W. *Polyhedron* **2011**, *30*, 1953.

(13) Sathyaraj, G.; Kiruthika, M.; Weyhermüller, T.; Nair, B. U. *Dalton Trans.* **2012**, *41*, 8460.

(14) Gao, F.; Chao, H.; Ji, L.-N. *Chem. Biodiversity* **2008**, *5*, 1962.

(15) (a) Han, M.-J.; Gao, L.-H.; Lu, Y.-Y.; Wang, K.-Z. *J. Phys. Chem. B* **2006**, *110*, 2364. (b) Fan, S.-H.; Zhang, A.-G.; Ju, C.-C.; Gao, L.-H.; Wang, K.-Z. *Inorg. Chem.* **2010**, *49*, 3752.

(16) Zhu, X.; Lu, W.; Zhang, Y.; Reed, A.; Newton, B.; Fan, Z.; Yu, H.; Ray, P. C.; Gao, R. *Chem. Commun.* **2011**, *47*, 10311.

(17) Hallett, A. J.; White, N.; Wu, W.; Cui, X.; Horton, P. N.; Coles, S. J.; Zhao, J.; Pope, S. J. A. *Chem. Commun.* **2012**, *48*, 10838.
(18) (a) Wu, W.; Ji, S.; Wu, W.; Shao, J.; Guo, H.; James, T. D.; Zhao, J. *Chem.—Eur. J.* **2012**, *18*, 4953. (b) Ji, S.; Guo, H.; Wu, W.; Wu, W.; Zhao, J. *Angew. Chem., Int. Ed.* **2011**, *50*, 8283.
(19) Mo, H.-J.; Shen, Y.; Ye, B.-H. *Inorg. Chem.* **2012**, *51*, 7174.
(20) White, E. H.; Harding, M. J. C. *J. Am. Chem. Soc.* **1964**, *86*, 5686.
(21) Wasserman, H. H.; Druckrey, E. *J. Am. Chem. Soc.* **1968**, *90*, 2440.
(22) Tomita, M.; Irie, M.; Ukita, T. *Biochemistry* **1969**, *8*, 5149.
(23) Sheu, C.; Kang, P.; Khan, S.; Foote, C. S. *J. Am. Chem. Soc.* **2002**, *124*, 3905.
(24) Davies, M. J. *Photochem. Photobiol. Sci.* **2004**, *3*, 17.
(25) Cui, Y.; Mo, H. J.; Chen, J. C.; Niu, Y. L.; Zhong, Y. R.; Zheng, K. C.; Ye, B. H. *Inorg. Chem.* **2007**, *46*, 6427.
(26) Cui, Y.; Niu, Y. L.; Cao, M. L.; Wang, K.; Mo, H. J.; Zhong, Y. R.; Ye, B. H. *Inorg. Chem.* **2008**, *47*, 5616.
(27) Mo, H. J.; Niu, Y. L.; Zhang, M.; Qiao, Z. P.; Ye, B. H. *Dalton Trans.* **2011**, *40*, 8218.
(28) Mo, H. J.; Wu, J. J.; Qiao, Z. P.; Ye, B. H. *Dalton Trans.* **2012**, *41*, 7026.
(29) Rillema, D.; Sahai, R.; Matthews, P.; Edwards, A.; Shaver, R.; Morgan, L. *Inorg. Chem.* **1990**, *29*, 167.
(30) Bond, A.; Haga, M. *Inorg. Chem.* **1986**, *25*, 4507.
(31) (a) Radziszewski, B. *Ber. Dtsch. Chem. Ges.* **1877**, *10*, 70. (b) Hayashi, T.; Maeda, K. *Bull. Chem. Soc. Jpn.* **1962**, *35*, 2057. (c) Sonnenberg, J.; White, D. M. *J. Am. Chem. Soc.* **1964**, *86*, 5685. (d) Kang, P.; Foote, C. S. *J. Am. Chem. Soc.* **2002**, *124*, 9629. (e) Hatano, S.; Abe, J. *Phys. Chem. Chem. Phys.* **2012**, *14*, 5855.
(32) Wasserman, H. H.; Lipschutz, B. H. In *Singlet Oxygen*; Wasserman, H. H., Murray, R. W., Eds.; Academic Press: New York, 1979; pp 430−510.
(33) Sprintschnik, G.; Sprintschnik, H. W.; Kirsch, P. P.; Whitten, D. G. *J. Am. Chem. Soc.* **1977**, *99*, 4947.
(34) Sun, Y.; Lutterman, D. A.; Turro, C. *Inorg. Chem.* **2008**, *47*, 6427.
(35) (a) Calvert, J. M.; Caspar, J. V.; Binstead, R. A.; Westmoreland, T. D.; Meyer, T. J. *J. Am. Chem. Soc.* **1982**, *104*, 6620. (b) Nakamaru, K. *Bull. Chem. Soc. Jpn.* **1982**, *23*, 2098.
(36) Van Houten, J.; Watts, R. J. *J. Am. Chem. Soc.* **1976**, *98*, 4853.
(37) Adarsh, N.; Avirah, R. R.; Ramaiah, D. *Org. Lett.* **2010**, *12*, 5720.
(38) Murasecco-Suardi, P.; Gassmann, E.; Braun, A. M.; Oliveros, E. *Helv. Chim. Acta* **1987**, *70*, 1760.
(39) Neckers, D. C. J. *J. Photochem. Photobiol., A* **1989**, *47*, 1.
(40) Manju, T.; Manoj, N.; Braun, A. M.; Oliveros, E. *Photochem. Photobiol. Sci.* **2012**, *11*, 1744.
(41) Takizawa, S.-Y.; Aboshi, R.; Murata, S. *Photochem. Photobiol. Sci.* **2011**, *10*, 895.
(42) Blessing, R. H. *Acta Crystallogr., Sect. A* **1995**, *51*, 33.
(43) Sheldrick, G. M. *SHELXS-97, A Program for Crystal Structure Solution*; Göttingen University: Göttingen, Germany, 1997.
(44) Sheldrick, G. M. *SHELXL-97, A Program for Crystal Structure Refinement*; Göttingen University: Göttingen, Germany, 1997.
(45) (a) Malecki, J. G. *Polyhedron* **2010**, *29*, 2489. (b) Malecki, J. G. *J. Coord. Chem.* **2011**, *64*, 390.
(46) (a) Abdel-Shafi, A. A.; Beer, P. D.; Mortimer, R. J.; Wilkinson, F. *J. Phys. Chem. A* **2000**, *104*, 192. (b) Bhattacharyya, K.; Das, P. K. *Chem. Phys. Lett.* **1985**, *116*, 326.
(47) Haga, M. *Inorg. Chim. Acta* **1983**, *75*, 29.
(48) Barigelletti, F.; Cola, L. D.; Balzani, V.; Hage, R.; Haasnoot, J. G.; Reedijk, J.; Vos, J. G. *Inorg. Chem.* **1989**, *28*, 4344.
(49) Sun, Y.; Ojaimi, M. E.; Hammitt, R.; Thummel, R. P.; Turro, C. *J. Phys. Chem. B* **2010**, *114*, 14664.
(50) Chen, Y.; Lei, W.; Jiang, G.; Zhou, Q.; Hou, Y.; Li, C.; Zhang, B.; Wang, X. *Dalton Trans.* **2013**, *42*, 5924.
(51) Tanlielian, C.; Wolff, C.; Esch, M. *J. Phys. Chem.* **1996**, *100*, 6555.
(52) William, B. C.; Harry, B. G. *J. Am. Chem. Soc.* **1997**, *119*, 11620.